Chemical Engineering Journal 200–202 (2012) 491–498

Contents lists available at SciVerse ScienceDirect

Chemical Engineering Journal

journal homepage: www.elsevier.com/locate/cej

Preparation and evaluation of alginate-assisted spherical resorcinol–formaldehyde resin beads for removal of cesium from alkaline waste

Charu Dwivedi [a], Amar Kumar [b], Kuttan Ajish Juby [a], Manmohan Kumar [a,*], Piaray Kishen Wattal [b], Parma Nand Bajaj [a]

[a] Radiation & Photochemistry Division, Bhabha Atomic Research Centre, Trombay, Mumbai 400 085, India
[b] Process Development Division, Bhabha Atomic Research Centre, Trombay, Mumbai 400 085, India

HIGHLIGHTS

- Synthesis of resorcinol–formaldehyde spherical resin beads.
- Use of bio-compatible calcium alginate beads as template.
- Characterization of the synthesized beads using TGA, UTM SEM and BET surface area analysis techniques.
- Application of the synthesized beads in removal of cesium ions from aqueous waste.
- Sorption and kinetic studies of cesium ion removal by radiotracer technique.

ARTICLE INFO

Article history:
Received 16 April 2012
Received in revised form 18 June 2012
Accepted 19 June 2012
Available online 28 June 2012

Keywords:
Sorption
Sorption kinetics
Equilibrium
Cesium removal
Resorcinol-formaldehyde

ABSTRACT

A novel method of synthesis of spherical resorcinol–formaldehyde resin was developed, using calcium alginate beads as template. Batch sorption experiments were carried out, to remove cesium ions from aqueous alkaline solutions, using the synthesized resin beads. The effect of operating variables, such as the initial cesium ion concentration, sodium ion concentration, and contact time, on the sorption of cesium ions was studied. Equilibrium data were found to fit better to Langmuir isotherm equation, with a monolayer sorption capacity of 490.2 mg/g, and the complete elution of the sorbed cesium ions was also possible. Sorption data were also analyzed in terms of both Lagergren first-order and pseudo second-order kinetic models, and were found to follow pseudo second-order kinetics at lower initial cesium ion concentration. The kinetic parameters were determined at different initial concentrations. The process mechanism was found to be complex, consisting of both film diffusion and intraparticle diffusion. Sorption data were also analyzed, using a Boyd plot, which confirmed that the rate-limiting step is the film diffusion.

1. Introduction

The management and disposal of radioactive waste is an issue relevant to almost all the countries. The radioactive waste is generated from the use of radioactive materials in industry and medicine sector, as well as from research and nuclear establishments. Among the various radionuclides present in the nuclear waste stream, ^{137}Cs is of special concern, because, along with ^{90}Sr, it constitutes a major source of heat in the nuclear waste. This radionuclide has a long half-life, and is a biological hazard [1]. So, its removal from the nuclear waste streams, before discharge to the environment, is necessary. A variety of methods, based on liquid/liquid extraction, solid/liquid extraction, ion-exchange processes, etc., have been proposed/used for the removal/recovery of ^{137}Cs from nuclear waste. Currently, the ion exchange has emerged as one of the most effective and attractive processes for the treatment of these cesium-bearing waste waters [2–7]. This process is flexible, simple, compact, efficient enough to achieve decontamination factors of several orders of magnitude, and does not require any hazardous organic solvent. Removal/recovery of cesium from different types of nuclear waste streams, using various types of materials, such as aluminosilicates, phosphates (like ammonium molybdophosphate (AMP)), ferrocyanides, hydrous oxides of multivalent cations, pillared clays, and resorcinol formaldehyde resin, has been previously studied by many researchers [8–13]. Among these, only resorcinol–formaldehyde (RF) resin has been considered as a satisfying option for removal of Cs^+ ions from highly alkaline media because of low-cost, safety, availability, selectivity, easy operation and efficiency considerations [14]. Moreover, the other

* Corresponding author. Tel.: +91 22 25593994; fax: +91 22 25505151.
E-mail address: manmoku@barc.gov.in (M. Kumar).

1385-8947/$ - see front matter © 2012 Elsevier B.V. All rights reserved.
http://dx.doi.org/10.1016/j.cej.2012.06.081

reported resins and selective extractants/ligands loose their potential under very high salt concentration (~5 M Na^+ ion) and high alkaline (>3 M) conditions of actual nuclear waste. RF resin has exceptionally high affinity for Cs^+ ions, which can be attributed to the presence of phenolic –OH group, which ionizes under high alkaline condition. The conventional method of synthesis of RF resin comprises the bulk polymerization of resorcinol and formaldehyde in alkaline medium, followed by crushing of the thus obtained big RF chunks into granules of desirable mesh size [15]. But, these grounded gel particles are of irregular shape, have broad particle size distribution, and exhibit poor column hydraulic behavior. These problems can be solved by using spherical resin material [16]. A number of publications, mostly in the form of patents exist in the literature describing the synthesis of spherical RF beads. Further, the alginate beads have been efficiently utilized as template to produce different sorbents in the bead form [17]. But, to the best of our knowledge, no one has reported its use for the synthesis of spherical RF beads. Here, we are reporting a new method of the synthesis of spherical RF resin beads, using preformed calcium alginate beads as a template material. Further, the results of the characterization and the cesium ion sorption experiments using the synthesized beads, are discussed.

2. Experimental

2.1. Materials

Resorcinol, formaldehyde (37% in methanol, AR grade), sodium hydroxide, sodium nitrate, and cesium nitrate, were obtained from Merck. Sodium alginate and calcium chloride were purchased from SD Fine Chemicals, India. RF grounded gel was obtained from Process Development Division, Bhabha Atomic Research Centre, Mumbai, India. All the other chemicals used were of analytical grade. Water obtained from Millipore-Q water purification system, with conductivity <0.3 μS/cm, was used in all the experiments.

2.2. Techniques

Optical microscope (OM) images of the RF beads were recorded in a digital Blue QX5 computer microscope. Scanning electron microscopy (SEM) was employed to observe microscopic morphology of the synthesized resin beads on AIS2100 SERON Tech. SEM from South Korea. Thermogravimetry (TG) was performed on Mettler Toledo (TG/DSC STAR^e System), at a heating rate of 10 °C/min, in N_2 atmosphere. The mechanical strength of the synthesised RF beads was tested, using a universal testing machine (UTM) (LRX plus). Brunauer–Emmett–Teller (BET) surface area of the RF beads was determined by N_2 adsorption–desorption measurement, using 'SORPTOMATIC 1990' analyzer, from CE Instruments Italy. Samples were out-gassed at 100 °C in vacuum, before the measurement. The gamma activity measurements were carried out in a well-type NaI (Tl) [ECIL] detector, connected to a single-channel analyzer.

2.3. Synthesis of RF beads

In order to synthesize RF beads, alginate template beads were first synthesized. For that, 2.0% (w/w) aqueous solution of sodium alginate was obtained, by dissolving 2.0 g of sodium alginate in 100 ml of water, which was then dropped into a 4% calcium chloride solution through a syringe needle of 0.8 mm internal diameter, forming gelified calcium alginate microspheres. These beads were kept overnight in the calcium chloride solution, for complete curing, and then, washed with water. Resorcinol formaldehyde pre-condensate was prepared by reacting resorcinol and formaldehyde in aqueous media, using $NaCO_3$ as a catalyst. An aqueous solution, with resorcinol: formaldehyde: catalyst in the molar ratio of 1:2:0.05, was prepared, and allowed to react till it attained a suitable viscosity. Then, the pre-formed water-swollen alginate beads were equilibrated with this RF pre-condensate solution, for 3 h, and then separated from the rest of the RF pre-condensate solution. When the water swollen calcium alginate beads were equilibrated with RF pre-condensate, the water present in the beads was almost completely exchanged with the RF pre-condensate. On curing of the RF pre-condensate inside the beads, a very hard and densely cross-linked 3D network of bulk RF in the form of beads was obtained which hardly retained any characteristics of the alginate template beads. The partial/complete leaching out of the small amount of alginate present in the beads, on interaction with the solution containing Na^+ ions will not affect its physical stability and structure. On the contrary, it would have enhanced its porosity. After complete curing at 105 °C, for 4 h, the brown-colored RF beads were obtained. These beads were in sodium form, and hence, were dark-colored. The synthesized resin beads were converted into hydrogen form, by contacting it with 0.5 M HNO_3 in a 3:1 ratio of liquid-to-resin volume, for 1 h, with occasional gentle shaking. After that, the resin beads were separated, and washed with water thoroughly, to remove any residual acid till pH of the washing became near neutral. This acid treatment brought the resin in light-colored hydrogen form. This hydrogen form of the resin was air-dried, and stored. It was used as such, without any further treatment, in all the sorption experiments. Fig. 1a and b represent the optical microscope images of the Alginate and the RF beads, confirming their spherical shape and almost uniform size distribution. The diameter of the beads is ~2 mm. Fig. 1c shows SEM image of the outer surface of the RF beads. On the surface itself, long connecting channel-like features are visible. These channels may provide better accessibility to the exchangeable site, which will ultimately lead to better sorption properties.

2.4. Sorption studies

^{134}Cs radiotracer ($T_{1/2}$ = 2.06 y; specific activity = 8.44 Ci/ml) was procured from the Board of Radiation and Isotope Technology (BRIT), Mumbai, India. The solution was further diluted to the required concentrations, as and when required. The batch capacities of the resin were determined, by shaking 0.05 g of RF resins with 5 ml of the $CsNO_3$ solution of appropriate concentration, containing ^{134}Cs radiotracer. The solutions were stirred well, using a mechanical shaker, for 4 h, which was found to be sufficient for attaining equilibrium. However, for studying the kinetics of sorption, the equilibration time was varied from 0 to 4 h. All the test solutions, containing cesium ions, were prepared in 0.1 M NaOH solutions, to maintain similar alkalinity of the solutions. After the equilibration, a small portion of the aqueous phase (1 ml) was separated, and taken for counting gamma activity. The gamma activity measurements were carried out in a well-type NaI (Tl) detector.

Equilibrium sorption capacity, q_e, in mg/g, was calculated, using the following equation:

$$q_e = \frac{(C_o - C_e)V}{m} \quad (1)$$

where C_o is the initial cesium ions concentration, C_e is the equilibrium cesium ion concentration, V is volume of the solution, and m is weight of the sorbent.

2.5. Sorption isotherm models

The analysis of the data is required to understand the sorption process, and design sorption-based separation process. The sorption isotherm models describe the interaction between the sorbate and the sorbent, and also represent the surface properties of the

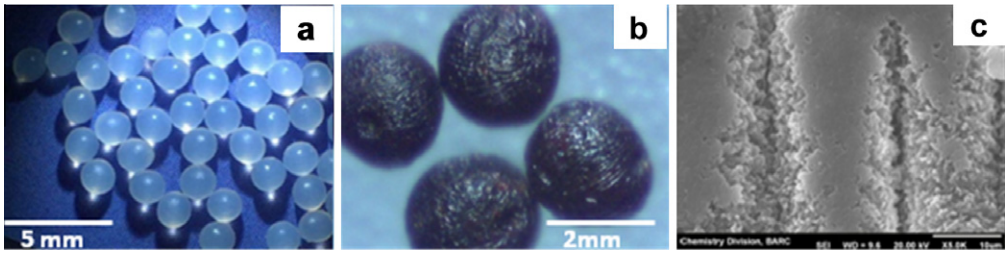

Fig. 1. Optical microscope images of: (a) alginate beads, (b) RF beads and (c) SEM image (at 5000×) of the outer surface of the RF beads.

sorbent. The sorption equilibrium provides fundamental physiochemical data for evaluating the applicability of the sorption process as a unit operation. In the present study, the equilibrium data were analyzed, using Freundlich and Langmuir isotherm expressions, given by the following equations [18,19]

$$\text{Freundlich isotherm}: \quad q_e = K_F C_e^{1/n} \tag{2}$$

where K_F is the Freundlich constant related to the sorption capacity, and n is the Freundlich parameter, which is indicative of heterogeneity of the sorbent surface.

$$\text{Langmuir isotherm}: \quad q_e = \frac{q_m K_L C_e}{1 + K_L C_e} \tag{3}$$

The linearized forms of the Freundlich and the Langmuir isotherm expressions can be written as follows:

$$\text{Freundlich isotherm}: \quad \log q_e = \log K_F + \frac{1}{n} \log C_e \tag{4}$$

$$\text{Langmuir isotherm}: \quad \frac{1}{q_e} = \frac{1}{q_m} + \frac{1}{K_L q_m C_e} \tag{5}$$

where q_m and K_L are the maximum monolayer capacity of the beads (mg/g), and the affinity constant, respectively. From the slope and the intercept of the plots of log (q_e) vs. log (C_e) and $1/q_e$ vs. $1/C_e$, the respective isotherm parameters can be determined.

2.6. Kinetic models

Kinetic models have been proposed to determine the mechanism of the sorption process, which provide useful data to improve the efficiency of sorption and feasibility of process scale-up [20]. Physical and chemical properties of the sorbents, as well as mass transfer processes, are some important parameters which determine/govern the sorption mechanism. In the present investigation, the sorption of the cesium ions onto RF beads was analyzed, using the pseudo first-order, pseudo second-order, and intraparticle diffusion models.

The Lagergren first-order kinetics model is given by the equation [21]

$$\frac{dq_t}{dt} = k_1(q_e - q_t) \tag{6}$$

where q_t (mg/g) is the amount of cesium ions sorbed at time t, and k_1 represents the sorption rate constant (min^{-1}). After integration and applying the boundary conditions, at $t = 0$, $q_t = 0$, the integrated form of the Eq. (6) becomes

$$\log(q_e - q_t) = \log(q_e) - \frac{k_1}{2.303} t \tag{7}$$

The values of k_1 and q_e can be determined from the slope and intercept, respectively, of the straight line plot of log ($q_e - q_t$) vs. t.

The kinetic data for the two initial cesium ion concentrations, 0.5 and 5 mM, were further analyzed, using a pseudo second-order relation proposed by Ho and McKay [22,23], which is represented by

$$\frac{dq_t}{dt} = k_2(q_e - q_t)^2 \tag{8}$$

where k_2 is the rate constant of the pseudo second-order sorption process (g mg^{-1} min^{-1}). After integration and applying the similar boundary conditions, the Eq. (8) can be rewritten as

$$\frac{t}{q_t} = \frac{1}{k_2 q_e^2} + \frac{1}{q_e} t \tag{9}$$

The above equation can be further simplified to Eq. (10), by substituting h in place of $k_2 q_e^2$, and the equation can be written as

$$\frac{t}{q_t} = \frac{1}{h} + \frac{1}{q_e} t \tag{10}$$

where h (mg g^{-1} min^{-1}) can be considered as the initial sorption rate, when $t/q_t \to 0$. The slope and the intercept of the plot of t/q_t vs. t give the values of q_e (mg/g) and h, respectively. Once h is known, the value of the constant k_2 (g/mg/min) can be determined.

The experimental data were also analyzed by the intraparticle diffusion kinetic model, to identify the steps involved during sorption. This model is described by external mass transfer and intraparticle diffusion. According to the Weber–Morris model, a plot of uptake q_t vs. the square root of time $t^{1/2}$ should be linear, if intraparticle diffusion is involved in the sorption system, and if these lines pass through the origin, then the intraparticle diffusion is the only rate-limiting step. The linear form of the intraparticle diffusion model equation can be represented as [24]

$$q_t = K_{id} t^{1/2} + I \tag{11}$$

where K_{id} (mg/g/$\text{min}^{1/2}$) is the intraparticle diffusion parameter and I (mg/g) gives an idea about the boundary layer thickness. To investigate the steps involved in the sorption process, the sorption data were also analyzed by the kinetic expression given by Boyd et al. [25]

$$F(t) = 1 - \frac{6}{\pi^2} \sum_{n=1}^{\infty} \frac{1}{n^2} \exp\left(-\frac{D_i \pi^2 t n^2}{r_o^2}\right) \tag{12}$$

$$F(t) = 1 - \frac{6}{\pi^2} \sum_{n=1}^{\infty} \frac{1}{n^2} \exp(-n^2 B t) \tag{13}$$

$$B = \frac{\pi^2 D_i}{r_o^2} \tag{14}$$

and F is the fractional attainment of equilibrium, i.e., the ratio of the solute sorbed at times t, to that at equilibrium ($F = q_t/q_e$), D_i the effective diffusion coefficient of the metal ions, r_o the radius of the sorbent and n is integer 1, 2, 3, ...

Solutions to the Eq. (13), depending on the value of F, are given as Eqs. (15) and (16) [26].

$$Bt = 2\pi - \frac{\pi^2 F}{3} - 2\pi\left(1 - \frac{\pi F}{3}\right)^{1/2} \quad (15)$$

$$Bt = -0.4977 - \ln(1 - F) \quad (16)$$

Thus, the value of Bt can be calculated for each value of F, using Eq. (15) for F values up to 0.85, and Eq. (16) for higher F values [26].

3. Results and discussion

3.1. Thermogravimetric analysis (TGA)

Thermo gravimetric analysis (TGA) of the synthesized beads was performed at a heating rate of 10 °C/min in nitrogen atmosphere, from ambient conditions up to 700 °C. TGA of the pure RF granule and the synthesized RF beads were carried out, using the material as prepared, without any pre-treatment, whereas that of the alginate beads was carried out, after just removing the surface water present on the swollen beads, using a filter paper. Fig. 2 shows typical TG profiles of the alginate, RF grounded gel and RF beads. The thermal degradation of the blank alginate beads occurs in two steps (Fig. 2, trace a). In the first step, (30–110 °C), there is a weight loss of ~62%, which may be due to the loss of the absorbed water. Then, an additional weight loss of 3.7%, due to thermal degradation of alginate is observed in the temperature range 200–700 °C. Fig. 2, trace b shows degradation of the RF grounded gel. The thermal decomposition of RF grounded gel does not have clear degradation steps, but only a gradual degradation profile. The weight loss (~9%) observed up to 110 °C may be due to the absorbed moisture. Then, a continuous weight loss is observed till the highest temperature investigated. TG profile of the RF beads (Fig. 2, trace c), too, has the same features as that of the RF grounded gel, and does not show any well-defined degradation steps. After heating up to 110 °C, a weight loss of ~ 9% is observed, which could be due to regained moisture. The TG profiles of the RF grounded gel and the RF beads are overlapping till 200 °C, and after that, a slightly more % weight loss is observed for the RF beads, as compared to that for the RF grounded gel in the temperature range of 200–473 °C. This could be due to the simultaneous decomposition of the alginate along with that of RF. But, at the end of 700 °C, about 46% of the total weight is left as charred residue in the case of RF, as compared to 41%, in the case of RF grounded gel. Similar nature of the TG profiles of the RF grounded gel particles and the synthesized RF beads indicates the presence of negligible amount of alginate in the synthesized beads.

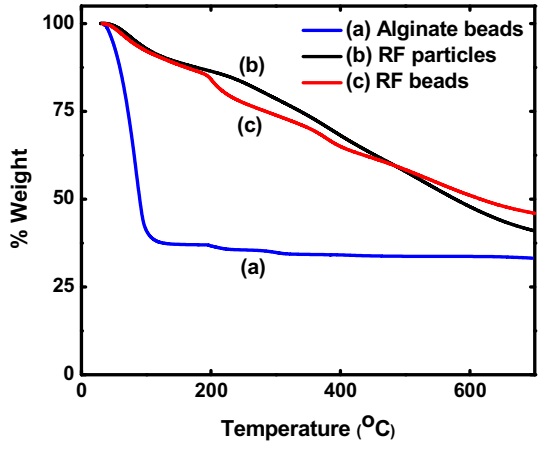

Fig. 2. TGA profile of: (a) Alginate beads, (b) RF particles and (c) RF beads.

3.2. Mechanical strength testing

Mechanical strength of the synthesized RF beads was tested, and compared with that of the conventional grounded RF gel particles, employing a universal testing machine, by applying the load in the range of 0–250 N, using 500 N load cell. Spherical RF beads showed first break at a load of 24–29 N, for the different samples tested, while for the grounded RF gel, breakage started at 2.5–5 N, and it showed different breakages in the range 2.5–15 N, depending on its shape and size. The irregular-sized grounded gel particles have some sharp and weak edges, which are the most susceptible for breaking under pressure, and results in generation of fine powder, which leads to column choking. While the synthesized RF beads are spherical in shape, and have better mechanical strength, as compared to the grounded RF resin gel particles currently in use, and, thus, are more appropriate for column operation..

3.3. Ion-exchange capacity and BET surface area

About 0.5 g of the H^+-form, air-dried RF resin beads were equilibrated with 100 ml of 0.1 M NaOH solution, containing 5% NaCl. The amount of NaOH consumed, was determined by the simple titration method, using a standard HCl solution and phenolphthalein indicator. From the amount of NaOH consumed, the total H^+–Na^+ ion-exchange capacity was determined to be 2.84 milliequivalents/g, i.e., 2.84 mmol/g of air-dried H^+form of RF resin. The specific surface area and pore volume of the beads were determined by BET N_2 adsorption method. The nitrogen adsorption-desorption isotherms were measured at 77 K and relative partial pressure (i.e. P/P_o) of N_2 of 0.98, after degassing the samples at 100 °C for 5 h. The surface area was found to be 568.45 m^2/g, and the pore volume was found to be 0.19 cc/g. This suggests that the surface area of the synthesized beads is very high, and supports the observations from SEM studies.

3.4. Effect of Na^+ ion concentration

The effect of Na^+ ion concentration on the amount of cesium ions sorbed was investigated over the Na^+ ion concentration range of 0.1 to 3.0 M, at a constant concentration of cesium ions. The concentration of Na^+ ions was varied, using $NaNO_3$ as a source of Na^+ ion. In this study, 5 ml solution of 0.02 M Cs^+ ions, in the presence of different concentrations of Na^+ ions, was agitated with 0.05 g of the RF beads, using bottle shaker (at a constant agitation speed of 50 RPM) at room temperature (30 °C), for 4 h, which was sufficient to attain equilibrium.

From Fig. 3, it is observed that uptake of cesium ions at 0.1 M Na^+ ion concentration is quite high, and then, it decreases sharply with increase in the Na^+ ion concentration up to 1 M. Thereafter, the q_e value is not affected much up to 2.0 M Na^+ ion concentration, and a q_e value of 46.47 mg/g is observed at higher Na^+ ion concentration of 3.0 M. These results indicate that the q_e value for cesium ion is affected by the presence of Na^+ ions in the solution due to the competitive sorption of Na^+ ions onto the available exchange sites. The observed q_e value of about 47 mg/g, even at the highest studied concentration of Na^+ ions, indicates that these beads can be efficiently utilized for removal of Cs^+ ions from the alkaline nuclear waste.

3.5. Effect of cesium ion concentration

The sorption capacity of the RF for cesium ions was determined by studying the sorption as a function of cesium ion concentration, at 300 K, in a batch experiment. The concentration of inactive cesium ions in the aqueous solution was increased from 5 to

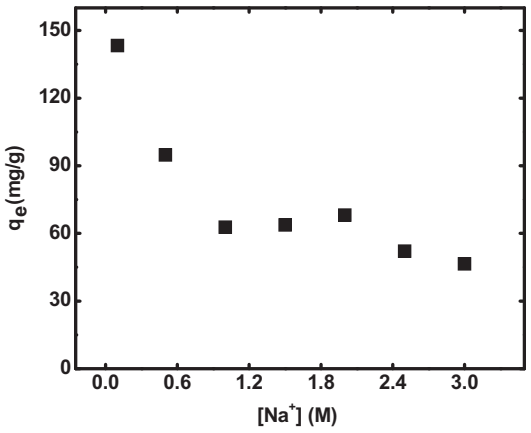

Fig. 3. Effect of Na^+ ion concentration on the removal of cesium ions at a constant cesium ion concentration of 0.02 M.

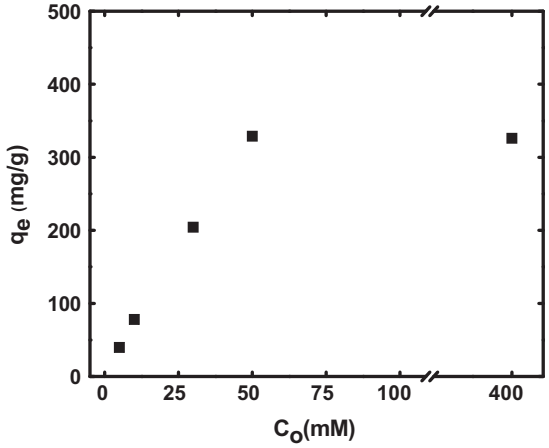

Fig. 4. Effect of the initial metal ion concentration on the sorption of Cs^+ ions onto the RF beads at 300 K.

400 mM, and the q_e was determined. It is observed that, initially, q_e increases linearly, with increase in Cs^+ ion concentration, because the active sites on the sorbent are sufficient, and the amount of cesium ions sorbed depends on the number of cesium ions transported from bulk to the sorbent. But, with further increase in the cesium ion concentration, the number of available active sites decreases and a deviation from linearity in the q_e vs. C_o plot is observed. An equilibration value of $\sim$ 326 mg/g, is obtained at 400 mM as shown in Fig. 4. The initial concentration provides an important driving force, to overcome all the mass transfer resistances to the Cs^+ ions between the aqueous and the solid phases. Therefore, a higher initial Cs^+ ion concentration will enhance the sorption process. The sorption capacity obtained for the synthesized RF beads is quite higher than that of RF-XAD beads reported earlier [16]. This could be due to the reason that unlike in RF-XAD beads, where RF was mostly present on the surface of the template XAD beads, the synthesized beads are almost pure RF resin beads.

The isotherm data were further analyzed, using Langmuir isotherm (Eq. (5)) and Freundlich isotherm models (Eq. (4)). Fig. 5a and b shows the equilibrium data fitted to Freundlich and Langmuir isotherm expressions, respectively. From these figures, it is observed that the equilibrium data fit to the Freundlich and Langmuir expressions, with a correlation coefficient values of 0.631 and 0.994, respectively. The higher correlation coefficient of 0.994 for the Langmuir isotherm shows that the sorption process conforms to the Langmuir isotherm, which predicts monolayer coverage of cesium on the RF resin. Table 1 gives the results of the fitting of the sorption data to the Langmuir and Freundlich isotherm models, after 4 h of equilibration.

Based on the Langmuir model, the maximum sorption capacity q_m (mg/g) of RF beads for cesium is 490.2 mg/g. The predicted Langmuir isotherm equation, for sorption of cesium onto RF, useful for design calculations, is given by

$$\text{Langmuir}: \quad q_e = \frac{23.04C_e}{1 + 0.047C_e} \tag{17}$$

3.6. Sorption Kinetics

Fig. 6 shows the effect of contact time on the removal of cesium ions at different initial metal ion concentrations. It is observed that the % removal of cesium ions decreases with increase in the initial metal ion concentration. For a contact time of 4 h, the % cesium ion removal decreases from 87.7% to 15.4%, for an increase in the initial Cs^+ ion concentration from 0.5 to 5 mM. Also, from the figure, it is observed that, at all the studied initial cesium ion concentrations, the rate of removal of Cs^+ ions is very rapid for the initial period of about 90 min, and thereafter, the sorption rate decreases, and finally, becomes negligible, after about 240 min. This is due to the combined effect of the decrease in flux (concentration gradient) with time due to transfer of the solute onto the solid phase, and availability of a fewer vacant sorption sites.

Fig. 7 shows the Lagergren plots (Eq. (7)) for two initial cesium ion concentrations of 0.5 and 5 mM. It is observed that Lagergren first-order kinetics model describes the sorption process well only for the first 90 min, at both the initial cesium ion concentrations, and thereafter, the sorption deviates from the model especially at the lower studied concentration. In other words, the sorption data are well represented only in the region where rapid sorption takes

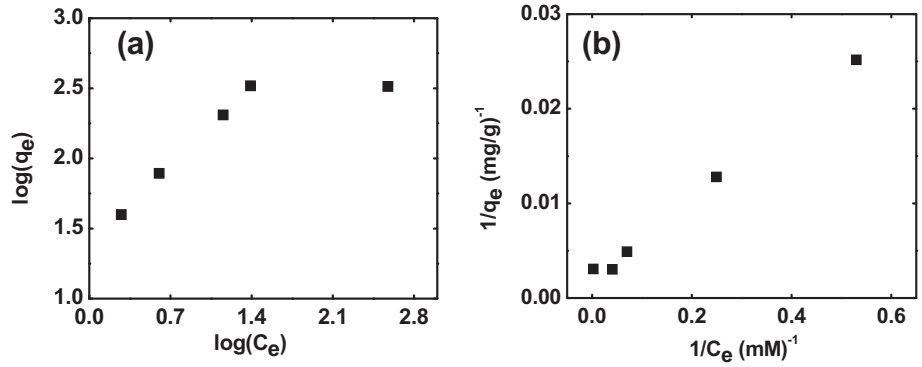

Fig. 5. (a) Freundlich and (b) Langmuir isotherm plots for sorption of Cs^+ ions onto the RF beads at 300 K.

Table 1
Sorption isotherm constants for cesium ions onto the RF beads.

K_F	$1/n$	$R^2_{(Freundlich)}$	K_L (L/mmol)	q_m	$R^2_{Langmuir}$
5.46	0.3902	0.631	0.047	490.2 mg/g	0.994

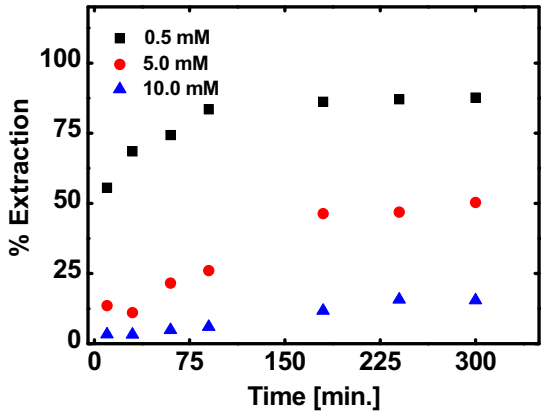

Fig. 6. The effect of equilibration time on the sorption of Cs^+ ions onto the RF beads at different initial Cs^+ ion concentrations.

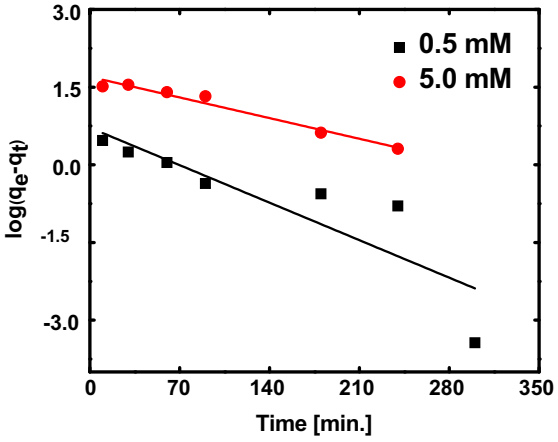

Fig. 7. Pseudo first-order plot for the sorption of Cs^+ ions onto the RF beads, at two different initial Cs^+ ion concentrations.

place, i.e., for the first 90 min. Ho and McKay [22], too, reported that the sorption data were represented well by the Lagergren first-order kinetic model only for the initial time period. This confirms that it may not be appropriate to use only the Lagergren first-order kinetics model, to describe the sorption of cesium ions onto RF resins for the entire sorption period and all the initial concentrations. The parameters and the coefficients obtained by employing pseudo first-order kinetic model to the experimental data are given in Table 2.

Fig. 8 shows the pseudo second-order plots, (Eq. (10)), for the sorption of cesium ions onto RF beads at the two different initial concentrations of cesium ions. The results show that, at lower initial cesium ion concentration, i.e., 0.5 mM, R_2^2 value is found to be higher than that for the pseudo first-order plot, whereas the R_2^2 value for the higher concentration (5 mM) is less than that for pseudo first-order plot. Moreover, the value of q_e calculated from the pseudo second-order plot is in agreement with the experimental q_e value of 7.93 mg/g at 0.5 mM initial cesium ion concentration. But, the q_e value calculated from the pseudo first-order plot is closer to that determined experimentally (45.3 mg/g) for 5 mM initial cesium ion concentration (Table 2). These observations suggest that the sorption system is explained best by pseudo second-order kinetics at the lower initial cesium ion concentration, but, at the higher initial cesium ion concentration, pseudo first-order kinetics is followed [23,24].

The intraparticle diffusion plots for the sorption of cesium onto RF beads, as given in Fig. 9, for different initial concentrations of cesium ions, show multilinearity. The first linear portion is, followed by a second linear portion, representing the different stages in the sorption, namely, external mass transfer, followed by intraparticle diffusion of the cesium ions onto the RF beads. The intraparticle diffusion parameter, K_{id}, at the two studied initial concentrations, is determined from the slope of the corresponding linear region of the Fig. 9, whereas the intercept of this second linear portion gives an idea about the boundary layer thickness. The calculated K_{id} and I values at different cesium concentrations are given in Table 2. As can be seen from the Fig. 9, the plot of q_e vs. $t^{1/2}$, for both the concentrations, is neither a straight line nor it passes through origin. This indicates some degree of boundary layer control, and also that, the intraparticle diffusion is not the only rate-limiting step, but other kinetic processes also may govern the rate of sorption, all of which may be operating simultaneously. Therefore, in order to find what the actual rate-controlling step, involved in the cesium sorption process, is, the sorption data were further analyzed by the kinetic expression given by Boyd et al. [25].

The values of Bt were calculated from Eq. (15), or Eq. (16), depending on the value of F. The calculated Bt values were plotted against time (figure not shown here). The linearity of this plot provides useful information to distinguish between the film diffusion and the intraparticle diffusion [26]. A straight line passing through the origin is indicative of sorption process governed by intraparticle-diffusion mechanism, otherwise, it is governed by film diffusion [27]. In the present case, the plots are non-linear, and do not pass through the origin, indicating that, the sorption process is of complex nature, consisting of both film diffusion and intraparticle diffusion steps, and film diffusion mainly is the rate-limiting process for the studied solute concentration range.

4. Desorption studies

Desorption experiments of the sorbed cesium ions were carried out using 0.5 M HNO_3. Firstly, 0.5 mM alkaline solution of cesium ions was equilibrated with the synthesized resin beads, for 4 h, keeping V/m ratio same as in other experiments. The sorbed cesium ions were then eluted by equilibrating the resin with

Table 2
Kinetic constants for the sorption of cesium ion onto the RF beads.

C_o (mM)	Pseudo first-order model			Pseudo second-order model			Intraparticle diffusion model	
	k_1, (min^{-1})	R_1^2	$q_{e,cal}$ (mg/g)	k_2, (g/(mg min))	R_2^2	$q_{e,cal}$ (mg/g)	K_{id} (mg/(g $min^{1/2}$))	I (mg/g)
0.5	0.024	0.71725	5.21	0.014	0.99961	8.23	0.032	7.44
5	0.013	0.96343	50.00	0.001	0.88068	61.65	4.392	13.01

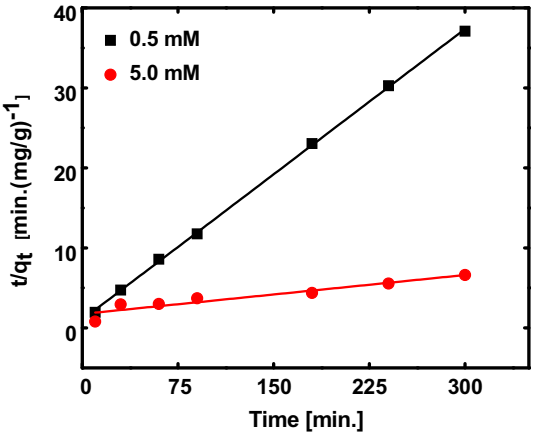

Fig. 8. Pseudo-second-order plot for cesium sorption onto the RF beads, at two different initial Cs^+ ion concentrations.

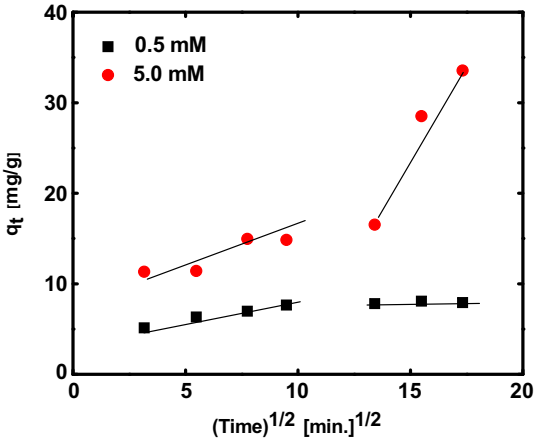

Fig. 9. Intra-particle diffusion plot for the Cs^+ ions sorption onto the RF beads at two different initial Cs^+ ion concentrations.

5 ml of 0.5 M HNO_3 solution, and the suitable aliquots of this solution were counted at different intervals of time. It was observed that, in ~10 min, 100% desorption of the sorbed cesium from the RF beads was achieved. This indicates that the beads can be regenerated, and complete recovery of the sorbed cesium is possible.

5. Conclusions

The present study describes a new method of synthesis of spherical RF beads of desired size, using calcium alginate beads as template. These synthesized RF resin beads can be used as sorbent for the removal of cesium ions from alkaline waste. The equilibrium data follow Langmuir isotherm, confirming the monolayer coverage of cesium onto RF particles. The monolayer capacity of the resin towards cesium ions from alkaline waste is quite high. Even in the presence of high sodium ion concentration, the resin shows reasonably good sorption capacity for cesium ions. Kinetics of the sorption of cesium ions onto RF beads is quite fast, and completes in ~4 h. The kinetic data obey pseudo second-order kinetics at lower concentration, but at higher concentration, the sorption is best explained by pseudo first-order kinetics model. Analysis of the mechanistic steps involved in the sorption process confirms the presence of multiple steps, including both film diffusion and intra-particle diffusion, with film diffusion as rate controlling step. These encouraging results suggest that the synthesized spherical RF resin beads can be used efficiently for removal of cesium ions from alkaline nuclear waste.

Acknowledgements

The author, Charu Dwivedi, is grateful to BRNS, Department of Atomic Energy, for awarding research fellowship. The authors are thankful to Dr. H. S. Sodaye, for SEM experiments. The authors also wish to acknowledge Dr. T. Mukherjee and Dr. S.K. Sarkar, for their encouragement during the course of the study.

References

[1] K. Stark, H.B.L. Pettersson, External radiation doses from ^{137}Cs to frog phantoms in a wetland area: in situ measurements and dose model calculations, Radiat. Environ. Biophy. 47 (4) (2008) 481–489.
[2] M.V. Ernest Jr, J.P. Bibler, R.D. Whitley, N.H.L. Wang, Development of a carousel ion-exchange process for removal of cesium-137 from alkaline nuclear waste, Ind. Eng. Chem. Res. 36 (7) (1997) 2775–2788.
[3] R. Harjula, J. Lehto, E.H. Tusas, A. Paavola, Industrial scale removal of cesium with hexacyanoferrate exchanger – process development, Nucl. Technol. 107 (3) (1994) 272–278.
[4] B.J. Hritzko, D.D. Walker, N.H.L. Wang, Design of a carousel process for cesium removal using crystalline silicotitanate, AIChE J. 46 (3) (2000) 552–564.
[5] J.D. Law, R.S. Herbst, T.A. Todd, Integrated AMP-PAN, TRUEX, and SREX testing. II. Flowsheet testing for separation of radionuclides from actual acidic radioactive waste, Sep. Sci. Technol. 37 (6) (2002) 1353–1373.
[6] E.H. Tusa, A. Paavola, R. Harjula, J. Lehto, Industrial scale removal of cesium with hexacyanoferrate exchanger – process realization and test run, Nucl. Technol. 107 (3) (1994) 279–284.
[7] J.R. Wiley, Decontamination of alkaline radioactive waste by ion exchange, Ind. Eng. Chem. Process Des. Dev. 17 (1) (1978) 67–71.
[8] B. Ma, S. Oh, W.S. Shin, S.-J. Choi, Removal of Co^{2+}, $Sr^{2+}$and Cs^+ from aqueous solution by phosphate-modified montmorillonite, Desalination 276 (2011) 336–346.
[9] M. Panagiotis, Application of natural zeolites in environmental remediation: a short review, Microporous Mesoporous Mater. 144 (1–3) (2011) 15–18.
[10] S. Inan, Y. Altaş, Adsorption of strontium from acidic waste solution by Mn–Zr mixed hydrous oxide prepared by co-precipitation, Sep. Sci. Technol. 45 (2) (2010) 269–276.
[11] S.P. Mishra, Vijaya, Removal behavior of hydrous manganese oxide and hydrous stannic oxide for Cs(I) ions from aqueous solutions, Sep. Purifi. Technol. 54 (1) (2007) 10–17.
[12] T. Möller, R. Harjula, A. Paajanen, Removal of ^{85}Sr, ^{134}Cs, and ^{57}Co radionuclides from acidic and neutral waste solutions by metal doped antimony silicates, Sep. Sci. Technol. 38 (12–13) (2003) 2995–3007.
[13] K. Shakir, M. Sohsah, M. Soliman, Removal of cesium from aqueous solutions and radioactive waste simulants by coprecipitate flotation, Sep. Purifi. Technol. 54 (3) (2007) 373–381.
[14] N.M. Hassan, K. Adu- Wusu, Cesium removal from Hanford tank waste solution using resorcinol–formaldehyde resin, Solvent Extr. Ion Exch. 23 (3) (2005) 375–389.
[15] S.K. Samanta, M. Ramaswamy, B.M. Misra, Studies on cesium uptake by phenolic resins, Sep. Sci. Technol. 27 (2) (1992) 255–267.
[16] C. Dwivedi, A. Kumar, J.K. Ajish, K.K. Singh, M. Kumar, P.K. Wattal, P.N. Bajaj, Resorcinol-formaldehyde coated XAD resin beads for removal of cesium ions from radioactive waste: synthesis, adsorption and kinetic studies, RSC Adv. 2 (13) (2012) 5557–5564.
[17] L. Liu, Y. Wan, Y. Xie, R. Zhai, B. Zhang, J. Liu, The removal of dye from aqueous solution using alginate–halloysite nanotube bead, Chem. Eng. J. 187 (2012) 210–216.
[18] D. Das, N. Das, L. Mathew, Kinetics, equilibrium and thermodynamic studies on biosorption of Ag(I) from aqueous solution by macrofungus *Pleurotus platypus*, J. Hazard. Mater. 184 (1–3) (2010) 765–774.
[19] K.R. Hall, L.C. Eagleton, A. Acrivos, T. Vermeulen, Pore- and solid-diffusion kinetics in fixed-bed adsorption under constant-pattern conditions, Ind. Eng. Chem. Fundam. 5 (2) (1966) 212–223.
[20] S. Eftekhari, A. Habibi-Yangjeh, S. Sohrabnezhad, Application of AlMCM-41 for competitive adsorption of methylene blue and rhodamine B: thermodynamic and kinetic studies, J. Hazard. Mater. 178 (1–3) (2010) 349–355.
[21] Y.S. Ho, G. McKay, The kinetics of sorption of basic dyes from aqueous solution by sphagnum moss peat, Can. J. Chem. Eng. 76 (4) (1998) 822–827.
[22] Y.S. Ho, G. McKay, The kinetics of sorption of divalent metal ions onto sphagnum moss peat, Water Res. 34 (2000) 735–742.
[23] S. Azizian, Kinetic model of sorption: a theoretical analysis, J. Colloid Interface. Sci. 276 (2004) 47–52.

[24] F.-C. Wu, R.-L. Tseng, R.-S. Juang, Characteristics of Elovich equation used for the analysis of adsorption kinetics in dye-chitosan systems, Chem. Eng. J. 150 (2–3) (2009) 366–373.
[25] G.E. Boyd, A.W. Adamson, L.S. Myers Jr, The exchange adsorption of ions from aqueous solutions by organic zeolites. II. Kinetics, J. Am. Chem. Soc. 69 (1947) 2836–2848.
[26] D. Reichenberg, Properties of ion-exchange resins in relation to their structure. III. Kinetics of exchange, J. Am. Chem. Soc. 75 (1953) 589–597.
[27] M. Sankar, G. Sekaran, S. Sadulla, T. Ramasami, Removal of diazo and triphenylmethane dyes from aqueous solutions through an adsorption process, J. Chem. Technol. Biotechnol. 74 (4) (1999) 337–344.